Atomic layer deposition of lanthanum oxide with heteroleptic cyclopentadienyl-amidinate lanthanum precursor - Effect of the oxygen source on the film growth and properties

Seppälä, Sanni

2018-08-30

Seppälä , S , Niinistö , J , Mattinen , M , Mizohata , K , Räisänen , J , Noh , W , Ritala , M & Leskelä , M 2018 , ' Atomic layer deposition of lanthanum oxide with heteroleptic cyclopentadienyl-amidinate lanthanum precursor - Effect of the oxygen source on the film growth and properties ' , Thin Solid Films , vol. 660 , pp. 199-206 . https://doi.org/10.1016/j.tsf.2018.06.011

http://hdl.handle.net/10138/238255
https://doi.org/10.1016/j.tsf.2018.06.011

Thin Solid Films 660 (2018) 199–206

Contents lists available at ScienceDirect

Thin Solid Films

journal homepage: www.elsevier.com/locate/tsf

Atomic layer deposition of lanthanum oxide with heteroleptic cyclopentadienyl-amidinate lanthanum precursor - Effect of the oxygen source on the film growth and properties

Sanni Seppälä[a,*], Jaakko Niinistö[a], Miika Mattinen[a], Kenichiro Mizohata[b], Jyrki Räisänen[b], Wontae Noh[c], Mikko Ritala[a], Markku Leskelä[a]

[a] Department of Chemistry, University of Helsinki, P.O. Box 55, FI-00014 Helsinki, Finland
[b] Division of Materials Physics, Department of Physics, University of Helsinki, P.O. Box 43, FI-00014 Helsinki, Finland
[c] AirLiquide Laboratories Korea, Yonsei Engineering Research Park, 50 Yonsei-ro, Seodaemun-gu, Seoul 03722, Republic of Korea

ARTICLE INFO

Keywords:
Atomic layer deposition
Lanthanum oxide
High-k oxides
Thin film
Hygroscopicity

ABSTRACT

La_2O_3 thin films were deposited by atomic layer deposition from a liquid heteroleptic La precursor, La(^{i}PrCp)$_2$(^{i}Pr-amd), with either water, ozone, ethanol, or both water and ozone (separated by a purge) as the oxygen source. The effect of the oxygen source on the film growth rate and properties such as crystallinity and impurities was studied. Saturation of the growth rate was achieved at 225 °C with O_3 as the oxygen source. With water, very long purge times were used due to the hygroscopicity of La_2O_3 but saturation of the growth rate was not achieved. Interestingly, when an O_3 pulse was added after the water pulse with a purge in between, the growth rate decreased and the growth saturated at 200 °C. With ethanol lanthanum hydroxide was formed instead of La_2O_3 at 200–275 °C whereas hexagonal La_2O_3 films were obtained at 300 °C but the growth was not saturative. Using the separate pulses of water and ozone in the same deposition provided the best results from the four studied deposition processes. After annealing the films deposited with the La(^{i}PrCp)$_2$(^{i}PrAMD)/H_2O/O_3 process showed pure hexagonal phase in all the films regardless of the deposition temperature, whereas mixtures of cubic and hexagonal La_2O_3 were seen with the other processes.

1. Introduction

Lanthanum oxide La_2O_3 is an interesting material for microelectronic applications due to its high permittivity (~27 for hexagonal La_2O_3) [1] and wide band gap (~5.5 eV) [2]. It has been studied as a gate dielectric on several semiconductors on its own [3–5] or combined with other oxides such as hafnium or yttrium oxide [6, 7]. La_2O_3 has also been used as a capping layer on Hf-based gate dielectric oxides [8–10]. Also, La_2O_3 and La containing ternary oxides have been studied as a passivation layer on Ge [11–13]. Another area of interest for La_2O_3 is optics because it is optically transparent over a wide wavelength range [14]. It can also be used as a dopant in thermoelectric oxide materials such as $CaMnO_3$ and $SrTiO_3$ to enhance electrical conductivity [15].

Although La_2O_3 is a technologically interesting material, it is somewhat problematic to process and study because of its hygroscopicity. When in contact with air, La_2O_3 absorbs water and forms lanthanum hydroxide, $La(OH)_3$, which has a low dielectric constant. In addition, the $La(OH)_3$ formation roughens the film surface which is a disadvantage in many applications [16]. To combat the moisture absorbance issue, ternary lanthanum containing oxides have been studied for microelectronic applications. One of the most studied is lanthanum aluminum oxide $LaAlO_3$ because it is moisture resistant and has thermal stability comparable to La_2O_3 [17–19].

With atomic layer deposition (ALD) it is possible to deposit accurately thin and conformal films without pinholes and hence ALD has become an attractive method for industrial use, especially in microelectronics [20]. ALD is a chemical method, where precursor vapors are pulsed onto a substrate one at a time and the film growth occurs only on the surface of the substrate in a self-limiting manner, enabling excellent controllability of the thickness and film composition.

Lanthanum precursors used in ALD include the β-diketonate La(thd)$_3$ (thd = 2,2,6,6-tetramethyl-3,5-heptane-dione) [21], cyclopentadienyl-based precursors such as La(Cp)$_3$ (Cp = cyclopentadienyl) [22] and La(^{i}PrCp)$_3$ (^{i}PrCp = isopropylcyclopentadienyl) [3, 23], amidinates La(^{i}PrAMD)$_3$ (^{i}PrAMD = *N,N′*-diiso-propylacetamidinato) [17] and La(^{i}PrfAMD)$_3$ (^{i}PrfAMD = *N,N′*-diisopropylformamidinato) [24] and silylamide La[N(SiMe$_3$)$_2$]$_3$ (N(SiMe$_3$)$_2$ = bis(trimethylsilyl) amide)

* Corresponding author.
E-mail address: sanni.seppala@helsinki.fi (S. Seppälä).

https://doi.org/10.1016/j.tsf.2018.06.011
Received 30 October 2017; Received in revised form 27 March 2018; Accepted 6 June 2018
Available online 07 June 2018

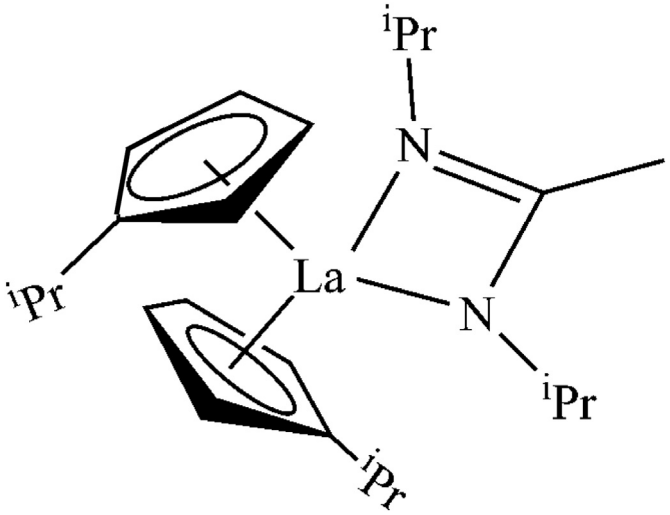

Fig. 1. Structure of the La(^{i}PrCp)$_2$(^{i}PrAMD) precursor.

[25]. La(thd)$_3$ with O_3 has a low growth rate of 0.36 Å/cycle at 225–275 °C. The process is saturative at 250 °C but at this temperature the films contain high amounts of carbon. La(^{i}PrCp)$_3$ is not very stable thermally and decomposition of the precursor is observed at 250 °C [26]. With La[N(SiMe$_3$)$_2$]$_3$/H_2O process saturation of the growth rate was not achieved and the films contained H and Si impurities. With the amidinate precursor La(^{i}PrfAMD)$_3$ saturation of the growth rate has been achieved at 250 °C with O_3 as the oxygen source with a growth rate of 1.0 Å/cycle. La(^{i}PrAMD)$_3$ has been used to deposit lanthanum aluminum oxide nanolaminates with trimethylaluminum and water.

The most studied oxygen sources in the deposition of La_2O_3 are H_2O and O_3, but also O_2 plasma has been used [23]. In La_2O_3 deposition the choice of oxygen source is more important than in most oxide processes because both water and ozone cause problems. The hygroscopicity of La_2O_3 complicates the process when water is used and with O_3 high levels of carbon impurities have been detected in the films due to carbonate formation [21].

In this paper, we report a heteroleptic liquid cyclopentadienyl-amidinate precursor, lanthanum bisisopropylcyclopentadienyl-*N*,*N*′-diisopropylacetamidinate, (La(^{i}PrCp)$_2$(^{i}PrAMD)) (Fig. 1) to be used as an La source in the ALD of lanthanum oxide. The aim of using heteroleptic precursors is to combine the best properties of the different types of ligands in order to tailor precursors with higher reactivity and thermal stability. Previously, we have reported ALD of Y, Pr, Gd and Dy oxides from the RE(^{i}PrCp)$_2$(^{i}PrAMD) (RE = rare earth) precursors with either water or ozone as the oxygen source [27]. In this study, we focus more on the effect of the oxygen source on the film properties. We tested the La precursor with H_2O and O_3 in separate deposition processes and both together in the same deposition process. Because of the problems assigned to water and ozone in the La_2O_3 deposition, ethanol was tested as an alternative oxygen source for comparison.

2. Experimental details

Films were deposited with an F-120 hot-wall flow-type ALD reactor (ASM Microchemistry, Ltd) using liquid La(^{i}PrCp)$_2$(^{i}PrAMD) precursor (Air Liquide) with either ethanol, water, ozone or both water and ozone (H_2O/O_3) as the oxygen source. When both H_2O and O_3 were used in the same deposition, the pulsing sequence was La precursor-purge-H_2O-purge-O_3-purge. Ethanol and water were kept at room temperature in containers outside the reactor and the vapor flow was controlled by needle valves. Pressure in the chamber was on the order of 5 mbar. Nitrogen (AGA, 99.999%, $H_2O \leq 3$ ppm, $O_2 \leq 3$ ppm) was used as the carrier and purging gas. Si(100) wafers were used as substrates. The La(^{i}PrCp)$_2$(^{i}PrAMD) precursor was evaporated at a temperature of 126 °C and the deposition temperature was in the range of 200–325 °C. Ozone with a concentration of 100 g/m^3 was generated from O_2 (AGA, 99.999%) in an ozone generator (Wedeco Modular 4 HC).

Films were characterized for thickness, crystallinity, morphology, and composition. Film thicknesses were determined by modeling [28] the reflectance spectra measured within wavelengths of 370–1100 nm with a spectrophotometer (Hitachi U-2000). Some thicknesses were confirmed also with X-ray reflectivity measurement (PANalytical X'Pert Pro MPD X-ray diffractometer). Crystallinity and phase of the films were determined by grazing incidence X-ray diffraction (GIXRD) using the same instrument and an incident beam angle of 1°. In situ high temperature XRD (HTXRD) measurements were conducted using an Anton-Paar HTK1200N oven. PANalytical Highscore Plus v.4.5 was used for XRD phase identification using ICDD and ICSD databases. Because of the air sensitivity of the films, they were stored in a desiccator. Surface morphology of the films was studied with a Multimode V atomic force microscope (AFM) equipped with a NanoScope V controller (Veeco Instruments) operated in the tapping mode. Images (500 × 500 nm^2 and 2 × 2 μm^2) were captured in air using silicon probes with a nominal tip radius of 8 nm and a nominal spring constant of 3 N/m (VLFM or FESP from Bruker). Roughness was calculated as a root-mean-square value (RMS) from 2 × 2 μm^2 images (512 × 512 pixels) obtained at 0.5–1.0 Hz scan rate. Roughness calculations and image processing were done with a Bruker Nanoscope Analysis 1.5 program. Film compositions were measured with time-of-flight elastic recoil detection analysis (TOF-ERDA) with 40 MeV $^{79}Br^{7+}$ beam obtained from a 5 MV tandem accelerator (EGP-10-II) at a detection angle of 40°. Some films were annealed at 700 °C in air or in N_2 atmosphere for 1 h. After the annealing the films were let to cool down slowly in the oven. XRD and TOF-ERDA were also measured from the annealed samples.

3. Results and discussion

In all four studied processes the growth rates increased with increasing deposition temperature. The highest growth rates were obtained with H_2O as the oxygen source (Fig. 2). Purge time had a clear effect on the growth rates when water was used. The growth rate varied from 1.2 Å/cycle at 200 °C to 3.0 Å/cycle at 300 °C when 0.8 s La precursor and H_2O pulses and 20 s purge after the water pulses were applied. With 10 s purge the growth rate was 4.4 Å/cycle already at 250 °C. The hygroscopicity of La_2O_3 can explain the very high growth

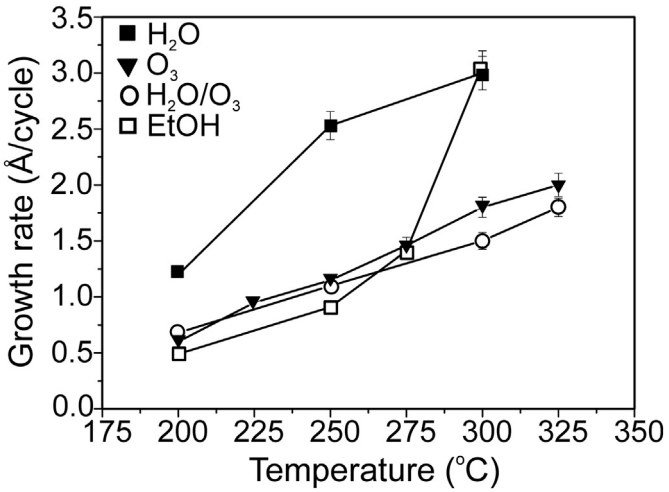

Fig. 2. Growth rates of the La_2O_3 films at different temperatures deposited with La(^{i}PrCp)$_2$(^{i}PrAMD)/H_2O (0.8 s precursor pulses, 20 s purge after H_2O), La(^{i}PrCp)$_2$(^{i}PrAMD)/O_3 (1.0 s pulses), La(^{i}PrCp)$_2$(^{i}PrAMD)/H_2O/O_3 (0.8 s La and H_2O pulses, 1.0 s O_3 pulse, 10 s purge after H_2O), and La(^{i}PrCp)$_2$(^{i}PrAMD)/EtOH processes (0.7 s pulses).

rates of the films deposited with H_2O as the oxygen source: $La(OH)_3$ is formed during the water pulse and if the purging period is not long enough, water is desorbed during the following La precursor pulse and reacts with the lanthanum precursor. This results in CVD-type reactions that do not enable the self-limiting growth mode of ALD [17]. When long purges after the water pulses are used, $La(OH)_3$ dehydrates before the next pulse. Lee et al. have reported that because of the hydroxide formation, very long (60 s), purge time after the water pulse was needed to achieve almost saturated growth with $La(^iPrfAMD)_3$ at 250 °C [24]. In our previous work [27], similar behavior was seen with praseodymium oxide but to a lesser extent as La is the most hygroscopic of the rare earths and the tendency decreases along the series. The chemistry of the light lanthanides resembles that of alkaline earth metals and similar behavior has been reported in ALD of barium oxide with water [29].

With O_3, the growth rates varied between 0.6 and 2.1 Å/cycle depending on the deposition temperature (Fig. 2). The pulse lengths for the precursors were 1.0 s and purges 1.5 s. When both water (0.8 s pulse) and ozone (1.0 s pulse) were used, the growth rates were close to the growth rates obtained with ozone as the only oxygen source. With the H_2O/O_3 process, growth rates varied from 0.7 Å/cycle at 200 °C to 1.8 Å/cycle at 325 °C. Two purge times after the water pulse, 10 and 20 s, were tested but the growth rate was nearly the same with both purge times, in marked contrast with the growth rates with water as the only oxygen source. It seems that the ozone pulse decreases the absorption of water in the growing film. This might be related to the carbon content of the films deposited with ozone as explained later.

Ethanol was tested as an oxygen source to see if it would have a lower reactivity than water toward $La(OH)_3$ formation. With ethanol, the growth rate followed the growth rates of O_3 and H_2O/O_3 200–275 °C. At 300 °C the growth rate was considerably higher compared to the lower deposition temperatures and was at the same level as with water at 300 °C (Fig. 2). Longer purge times after the ethanol pulse did not affect the growth rate of the films at 250 °C but at 300 °C the growth rate increased with increasing purge time. This is the opposite of what happens with water. Due to the abrupt change in the growth rate at 300 °C, we believe that water is formed during the deposition at 300 °C through dehydration of ethanol. Catalytic activity of metal oxide surfaces toward dehydration reactions of alcohols has been demonstrated for different metal oxides in various studies [30–33]. The formation of water is also supported by the hydrogen depth profiles measured by ERDA (not shown) since in the films deposited at 200 and 250 °C the hydrogen content is highest at the film surface and decreases deeper in the film whereas in the film deposited at 300 °C the hydrogen content is high through the whole film thickness.

Saturation of the growth rate was studied at 200 and 250 °C with water as the oxygen source but was not achieved even with the 20 s purge time after the H_2O pulse. With a 0.7 s La precursor pulse at 200 °C the growth rate was 1.2 Å/cycle and with a 2.5 s pulse already 3.2 Å/cycle. In the $La(^iPrCp)_2(^iPrAMD)/O_3$ process the saturation of the growth rate was confirmed at 225 °C with 1.0 Å/cycle (Fig. 3a) and in the $La(^iPrCp)_2(^iPrAMD)/H_2O/O_3$ process at 200 °C with 0.7 Å/cycle (Fig. 3b). With ethanol saturation was not achieved at any studied temperature: At 200 °C the growth rate varied between 0.90 Å/cycle with 0.7 s La precursor pulse and 2.8 Å/cycle with 3.0 s pulse.

The choice of the oxygen source affected the crystallinity of the films. The films deposited with ozone at 200 °C were amorphous and at 225–275 °C very weakly crystalline. Cubic, *c*, La_2O_3 (ICDD-022-0367) was obtained at 300 °C and a mixture of cubic and hexagonal, *h*, La_2O_3 (ICDD-005-0602) at 325 °C (Fig. 4a). Previously, with the $La(thd)_3/O_3$ process amorphous films were reported below 300 °C and cubic La_2O_3 at and above 300 °C [21]. The $La(^iPrCp)_3/O_3$ process produced amorphous films at 200 °C [3]. In the $La(thd)_3/O_3$ study, the amorphous films were identified by TOF-ERDA to contain large amounts of carbon and the elemental composition was close to $La_2O_2CO_3$ phase. Also in our work, high carbon contents were measured from the films deposited with ozone at low temperatures, which can explain the amorphous nature of these films. The elemental compositions will be discussed later in the text.

With water, crystalline La_2O_3 films were deposited at 200 °C and above. The films deposited at 200–250 °C were mixtures of the cubic and hexagonal phases but the hexagonal phase became more dominant with increasing deposition temperature (Fig. 4b). At 300 °C the cubic phase was dominant again. It appears that the phase composition of La_2O_3 films may depend in a sensitive manner on both deposition temperature and impurity contents. In the previous studies with water as the oxygen source, amorphous films were deposited at all the studied temperatures from 150 to 250 °C in the $La[N(SiMe_3)_2]_3/H_2O$ process, apparently because of the high amounts of Si impurities in the films [25]. The films deposited with the $La(Cp)_3/H_2O$ process at 260 °C were reported to contain LaO(OH) according to Fourier transform infrared spectroscopy. The data was measured 5 min after the film was taken out of the reactor. XRD measurement was not reported [22].

The crystallinity of the films deposited with the H_2O/O_3 process resembled the films deposited with ozone at 200–275 °C (Fig. 4c). The films were amorphous at 200 °C and weak crystallinity was observed at 250 and 275 °C. Above that the films were cubic La_2O_3. At 300 °C the most intensive peak was (004) but at the higher deposition temperature of 325 °C (222) was clearly the strongest. Unlike with water or ozone alone, no mixtures of phases were formed at any deposition temperature.

The film deposited with ethanol at 250 °C showed very clear peaks from hexagonal $La(OH)_3$ (ICDD-036-1481) instead of La_2O_3 (Fig. 4d). There were also some weakly visible peaks that could be attributed to *c*-La_2O_3. Some of the hydroxide reflections were also visible at 200 °C but the peaks were very broad with low intensities. The presence of both the hydroxide and oxide phases is supported by the results of the compositional analysis discussed later. At 275 °C, a mixture of *h*-La_2O_3 and $La(OH)_3$ phases with low intensities and broad peaks was observed. At 300 °C the diffraction peaks match h-La_2O_3 but the two strongest ones are not fully separated indicating a small $La(OH)_3$ peak in between (Fig. 4d).

Differences in the crystal structures between the films deposited with different processes were visible also after annealing at 700 °C in air. In the case of O_3, the originally amorphous films deposited at 250 °C crystallized to the cubic La_2O_3 phase with a couple of very small peaks attributed to the hexagonal phase while the film deposited at 325 °C had the strongest peaks from the hexagonal phase but also a minor peak from the cubic phase was visible (Fig. 5a). Films deposited with H_2O above 200 °C were hexagonal La_2O_3 after the annealing while the film deposited at 200 °C was still a mixture of cubic and hexagonal phases (Fig. 5b). Films deposited with H_2O/O_3 above 250 °C were hexagonal La_2O_3 after the annealing (Fig. 5c). At 250 °C one very small peak attributed to cubic La_2O_3 was observed after the annealing. With ethanol, the $La(OH)_3$ containing films deposited at 200 and 250 °C were converted to mixtures of different phases (Fig. 5d). Hexagonal La_2O_3 was seen clearly with strong peaks but in addition there seemed to be LaO(OH) (ICDD-019-0656) and at least at 250 °C also cubic La_2O_3. Annealing at 700 °C in air atmosphere is thus not enough to remove all the hydroxide species from these films. In contrast, the film deposited at 300 °C was *h*-La_2O_3 after the annealing.

The films deposited with O_3 or H_2O/O_3 at the temperatures where the growth rates saturated had the highest carbon contents as deposited and after annealing at 700 °C in air there were some additional peaks that did not fit the La_2O_3 phases, although the compositional analysis showed low carbon content. These peaks were attributed to lanthanum silicate phases. HTXRD in air from room temperature to 900 °C confirmed that there is no such temperature where the oxide phase would be the only phase. When the peaks from the carbonate phase disappeared, new peaks from the silicate phases appeared. This behavior is very different from the films deposited at higher temperatures. However, annealing in nitrogen atmosphere was successful. Both the

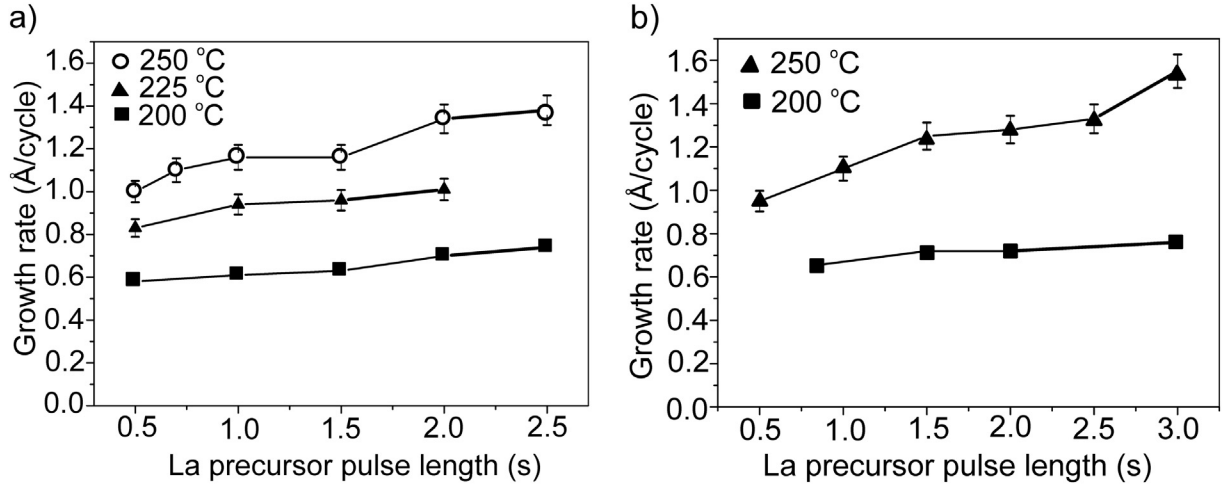

Fig. 3. La_2O_3 film growth rate as a function of La precursor pulse length in a) La(^{i}PrCp)$_2$(^{i}PrAMD)/O_3 and b) La(^{i}PrCp)$_2$(^{i}PrAMD)/H_2O/O_3 process. Pulse time for H_2O was 0.8 s and for O_3 1.0 s.

film deposited with ozone and the film deposited with water and ozone at 200 °C crystallized to cubic La_2O_3 at 500 °C. At 600 °C the first sign of the hexagonal phase was seen and at 750 °C the film deposited with H_2O/O_3 was pure hexagonal La_2O_3 whereas the film deposited with O_3 was hexagonal La_2O_3 with one very small peak from the cubic phase. According to the HTXRD measurements, these films can be crystallized to either cubic or hexagonal La_2O_3 by carefully choosing the annealing temperature (Fig. 6).

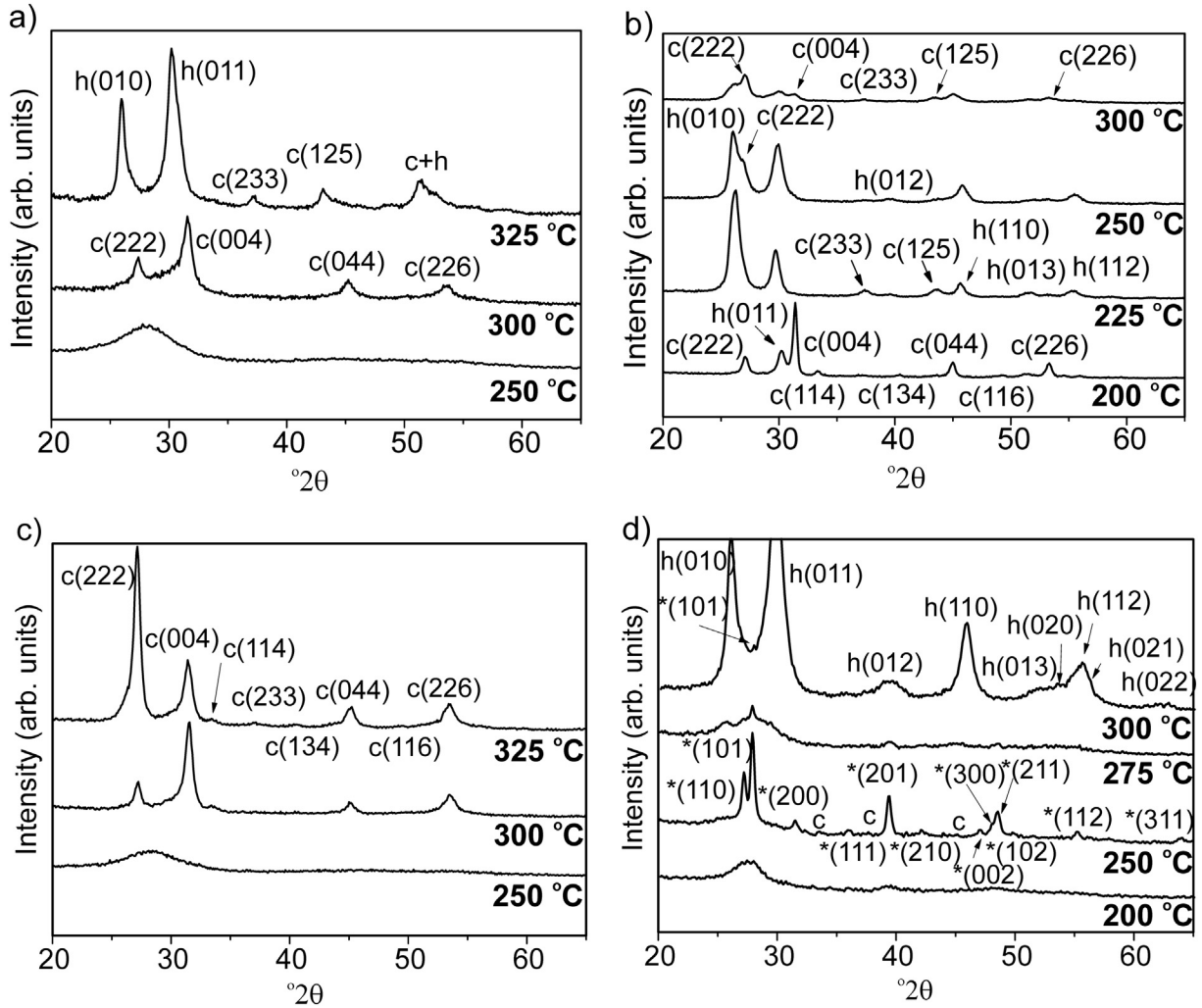

Fig. 4. XRD patterns of the as-deposited La_2O_3 films deposited with a) O_3 b) H_2O, c) H_2O/O_3 and d) EtOH as the oxygen source. *h* is hexagonal and *c* cubic La_2O_3, * is hexagonal $La(OH)_3$.

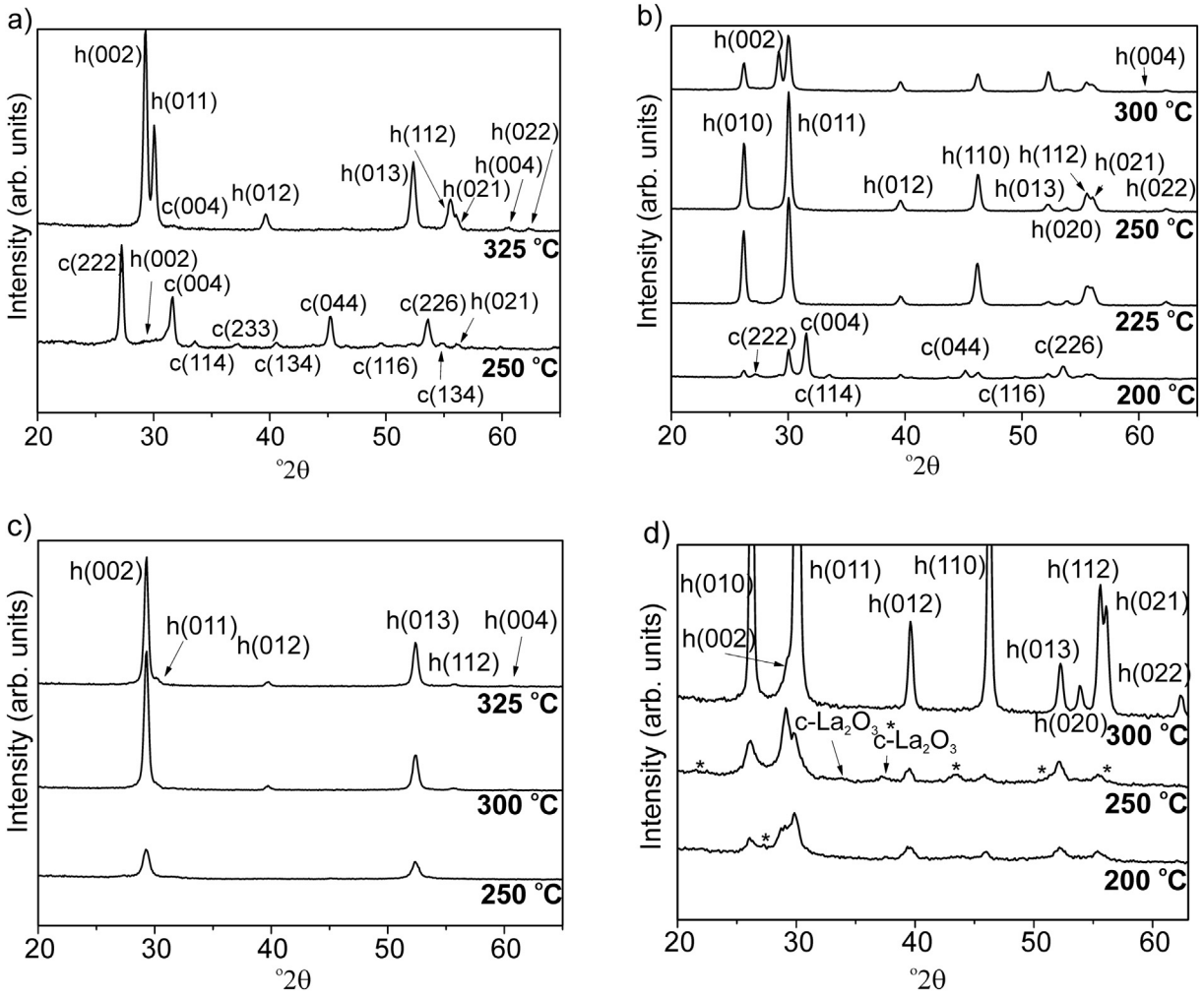

Fig. 5. XRD patterns of the films annealed at 700 °C for 1 h in air deposited with a) O_3 b) H_2O, c) H_2O/O_3 and d) EtOH as the oxygen source. * in figure d is LaO(OH).

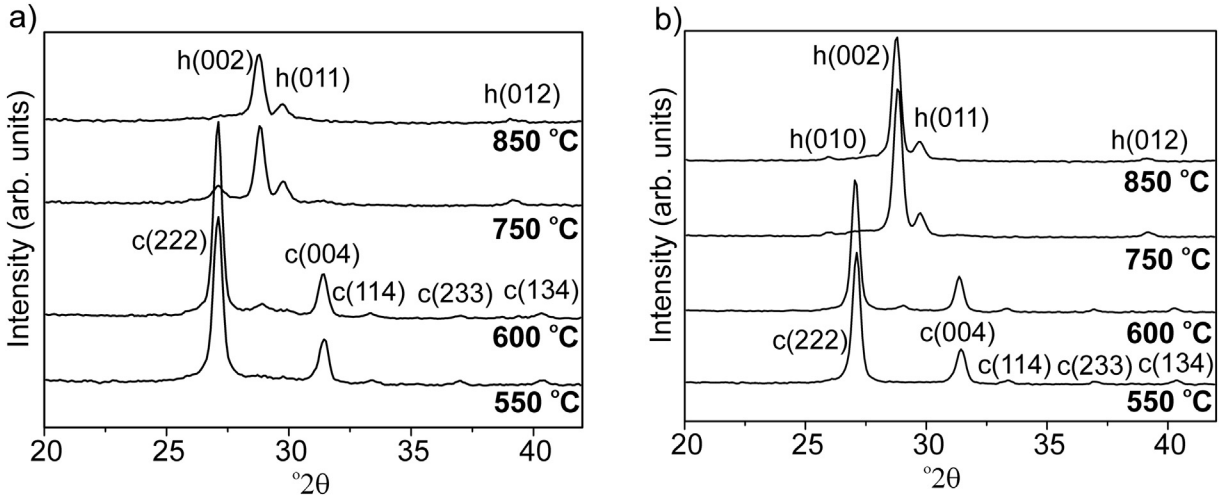

Fig. 6. HTXRD patterns of films deposited at 200 °C with a) O_3 and b) H_2O/O_3 as the oxygen source. The measurements were done in N_2 atmosphere.

Previously, it has been reported that the thickness of the films might affect the appearance of the pure hexagonal phase. For example, in the case of the $La(Cp)_3/H_2O$ process, the pure hexagonal phase appeared in films thicker than 100 nm [1]. This thickness could be decreased by using ozone instead of water as the oxygen source [34]. In our study, a 110 nm thick film deposited with ozone as the oxygen source was a mixture of cubic and hexagonal phases after annealing. With water, the deposition temperature affected the phase: > 100 nm thick film deposited at 200 °C was still a mixture of phases after annealing but > 100 nm thick films deposited at 225 and 250 °C were hexagonal La_2O_3 after annealing. The $La(^iPrCp)_2(^iPrAMD)/H_2O/O_3$ process was clearly different since the annealed films showing hexagonal phase at all

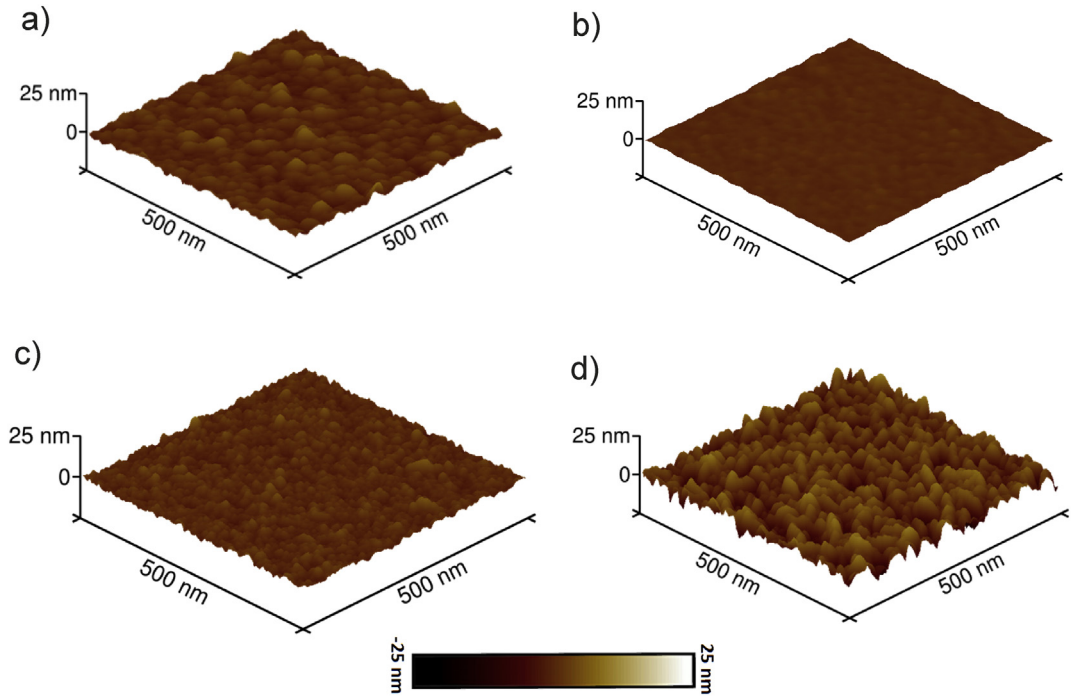

Fig. 7. AFM images of the films deposited at 250 °C with a) H_2O b) O_3, c) H_2O/O_3 and d) EtOH as the oxygen source. Film thicknesses were 47–65 nm.

deposition temperatures were only 47–72 nm thick. When exposed to air at room temperature, the annealed films started to convert to hydroxide faster than the as-deposited films indicating better film purity as discussed below.

The AFM images of the films deposited at 250 °C (Fig. 7) and 300 °C (Fig. 8) indicate that the films deposited with water are rough (RMS roughness values above 2 nm) compared to the films deposited with O_3 or H_2O/O_3. The high roughness values are likely due to the high growth rates and crystallinity of the films. The films deposited with ozone as the oxygen source were the smoothest with RMS values ranging from 0.61 nm at 200 °C to 0.91 nm at 300 °C. The roughness increases with increasing deposition temperature which can be explained by the increasing crystallinity. For the H_2O/O_3 process the roughness values were around 1.5 nm for all the measured films. The films deposited with the La(^{i}PrCp)$_2$(^{i}PrAMD)/EtOH process at 200 and 250 °C were $La(OH)_3$ and the roughness values of these films were much higher than the values of the La_2O_3 films from the other processes. A 55 nm thick $La(OH)_3$ film deposited at 250 °C had RMS value of 3.8 nm. At 300 °C also the films deposited with EtOH were La_2O_3 and the roughness was 1.6 nm which is in the same range with the H_2O/O_3 process.

Elemental compositions of selected films were measured with TOF-ERDA. The main impurities were carbon and hydrogen. However, the hydrogen contents are not completely representative because the films react with moisture to form hydroxide during storage. A general trend

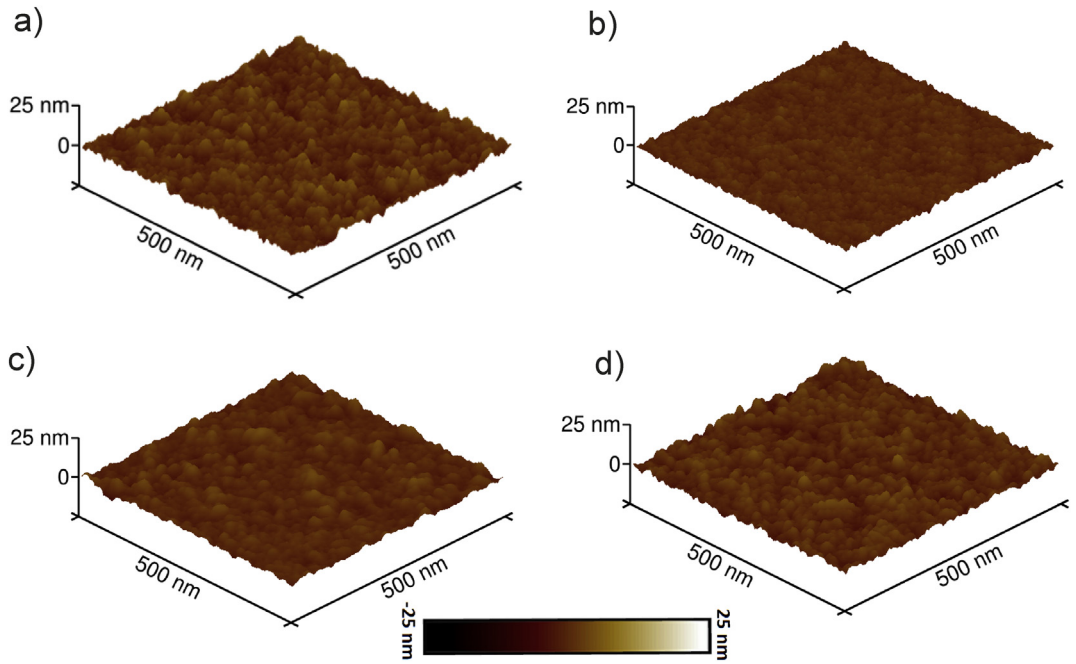

Fig. 8. AFM images of the films deposited at 300 °C with a) H_2O b) O_3, c) H_2O/O_3 and d) EtOH as the oxygen source. Film thicknesses were 36–72 nm.

Table 1
Representative samples from the depositions with different oxygen sources.

Oxygen source	Growth rate saturation	La:O	C (at. %)	H (at. %)	Crystalline phase
H_2O/O_3 at 200 °C	Yes	0.45	8	3	Amorphous
Annealed at 700 °C in N_2		0.51	0.2	6	*h*
O_3 at 200 °C	Yes	0.31	19	3	Amorphous
Annealed at 700 °C in N_2		0.53	0.2	7	*h*, minor peaks *c*
H_2O at 250 °C	No	0.51	2	24	*h*, minor peaks *c*
Annealed at 700 °C in air		0.60	0.5	2	*h*
EtOH at 300 °C	No	0.54	3	22	*h*, minor La $(OH)_3$
Annealed at 700 °C in air		0.60	0.2	2	*h*

h hexagonal La_2O_3, *c* cubic La_2O_3.

seemed to be that the higher the carbon content the lower the hydrogen content. The highest carbon levels were measured from the films deposited at low temperature with ozone (19 at.% of carbon at 200 °C and 10 at.% at 250 °C) and the second highest from the films deposited with H_2O/O_3 (around 8 at.% of carbon at 200–250 °C). All of these films contained around 3 at.% of hydrogen. When the deposition temperature was raised, the carbon content decreased and hydrogen content increased. For example with H_2O/O_3 at 325 °C the carbon content was < 4 at.% and the hydrogen content 6 at.%, and with ozone the numbers were 4 at.% of carbon and 15 at.% of hydrogen.

Previously, high carbon levels have been detected in the $La(thd)_3/O_3$ process with around 11 at.% of carbon at deposition temperatures of 225–300 °C [21]. Lanthanum oxide is known to be very hygroscopic but these results imply that carbonate impurities stabilize the films, i.e. the high carbon content inhibits the absorption of moisture and keeps the hydrogen content lower in the films deposited with ozone and H_2O/O_3 at 200 to 250 °C. Visually, the films with high carbon content maintained their original appearance when stored in air whereas the films deposited with water started to turn matt and eventually flaked off the substrate.

With the water and ethanol processes, the carbon levels in the films were clearly lower and hydrogen levels higher than with ozone and H_2O/O_3, between 1 and 2 at.% of carbon and 11 to 24 at.% of hydrogen at 200–250 °C. This can be explained by the strong oxidation ability of ozone which can cause bonds in the ligands to break, leaving carbon impurities in the film. The films deposited with EtOH at 250 °C showed mainly $La(OH)_3$ in the X-ray diffractograms and very small peaks that could be due to cubic La_2O_3. According to the compositional analysis, the hydrogen content of this film is 17 at.%. If the whole film would be $La(OH)_3$, the hydrogen content should be much higher, 43 at.%. This result confirms that the very small peaks seen in the XRD are La_2O_3. It is also possible that part of the film is amorphous. Even though the film deposited at 300 °C with EtOH shows h-La_2O_3 in XRD it contains 22 at. % of hydrogen according to TOF-ERDA.

All measured films had an excess of oxygen compared to the stoichiometric La:O ratio (0.67) in La_2O_3. The best La:O ratios in our study (~0.55) were measured from the films deposited with water and the worst with ozone as the oxygen source. With water the ratios did not change with the deposition temperature as much as they did with ozone (0.31 at 200 °C and 0.47 at 325 °C). The excess of oxygen is explained with the carbonate and hydroxyl species in the films.

Some films contained small amounts of fluorine (from 0.06 ± 0.3 to 0.75 ± 0.2 at.%) and nitrogen (max. 0.15 ± 0.1 at.%). Fluorine has been seen before in films deposited with ozone in the same type of ALD reactor and it is attributed to the fluorine containing gaskets and vacuum grease used in the reactor [35]. An obvious source for the nitrogen is the amidinate ligand.

Compositional analysis was performed for selected films also after annealing at 700 °C. To minimize the contamination caused by reactions with ambient air, the films were taken to the TOF-ERDA measurement right after the annealing. The carbon contents of the films annealed in air were in general < 1 at.% while the highest value was 2 at.% in a film deposited at 250 °C with H_2O/O_3. The hydrogen contents varied between 2 and 5 at.%. The films deposited with EtOH at 200 and 250 °C showed LaO(OH) phase in the XRD. According to the TOF-ERDA depth profiles, the LaO(OH) phase is probably the topmost layer since there is around 10 at.% of hydrogen close to the surface but only around 2 at.% deeper in the bulk of the films. Also chlorine (~0.5 at.%) was found from the annealed samples and it is most likely contamination from the oven used to anneal the samples.

The films deposited with O_3 or H_2O/O_3 at 200 °C and annealed at 700 °C in N_2 atmosphere contained only 0.2 at.% of carbon and 6–7 at. % of hydrogen according to the compositional analysis. The La:O ratios (0.53 for O_3 and 0.51 for H_2O/O_3) were closer to the stoichiometric value than after annealing in air atmosphere (0.41 for both processes) but still there was some additional oxygen, apparently in the form of hydroxide.

4. Conclusions

In this work, we studied atomic layer deposition of La_2O_3 from a heteroleptic La precursor $La(^iPrCp)_2(^iPrAMD)$ with either H_2O, O_3, EtOH, or both H_2O and O_3 as the oxygen source. The choice of the oxygen source had a great effect on the growth rates, crystallinity, and impurity levels of the films. With water, the hygroscopicity of La_2O_3 caused problems and saturation of the growth rate was not achieved even when 20 s purge period after the water pulse was used. Interestingly and importantly, hygroscopicity was not a problem when ozone pulse was added after the water pulse since saturation of the growth rate was achieved with the $La(^iPrCp)_2(^iPrAMD)/H_2O/O_3$ process at 200 °C with a growth rate of 0.7 Å/cycle. Also the $La(^iPrCp)_2(^iPrAMD)/O_3$ process was saturative at 225 °C with a growth rate of ~1 Å/cycle. At 250 °C both of these processes were close to saturation. With ethanol, no saturation was achieved at any deposition temperature. Besides La_2O_3, lanthanum hydroxide $La(OH)_3$ was formed when ethanol was the oxygen source. Evidence of the hydroxide formation was not seen in the diffractograms of the other processes, although elemental analysis revealed that the films deposited with water had high hydrogen content. The $La(^iPrCp)_2(^iPrAMD)/H_2O/O_3$ process showed deviating crystallization behavior from the other processes after annealing as pure, high permittivity hexagonal phase was formed in all the films regardless of the deposition temperature, whereas the films deposited with the other processes had mostly mixtures of cubic and hexagonal La_2O_3. The most representative samples from each process are collected in Table 1.

Acknowledgment

Mr. Mikko Heikkilä is thanked for the help with the XRD measurements and Dr. Peter King for correcting the English in the manuscript. This work was funded by the Finnish Centre of Excellence in Atomic Layer Deposition (Academy of Finland), (284 623).

References

[1] G. Scarel, A. Debernardi, D. Tsoutsou, S. Spiga, S.C. Capelli, L. Lamagna, S.N. Volkos, M. Alia, M. Fanciulli, Vibrational and electrical properties of hexagonal La_2O_3 films, Appl. Phys. Lett. 91 (2007) 102901.
[2] G. Scarell, A. Svane, M. Fanciulli, Scientific and technological issues related to rare earth oxides: an introduction, in: M. Fanciulli, G. Scarell (Eds.), Rare Earth Oxide Thin Films: Growth, Characterization and Applications, Springer – Verlag, Berlin, Heidelberg, 2007, pp. 1–13.
[3] L. Lamagna, C. Wiemer, M. Perego, S.N. Volkos, S. Baldovino, D. Tsoutsou, S. Schamm-Chardon, P.E. Coulon, M. Fanciulli, O_3 -based atomic layer deposition of hexagonal La_2O_3 films on Si(100) and Ge(100) substrates, J. Appl. Phys. 108 (2010)

084108.
[4] H. Oomine, D.H. Zadeh, K. Kakushima, Y. Kataoka, A. Nishiyama, N. Sugii, H. Wakabayashi, K. Tsutsui, K. Natori, H. Iwai, Electrical characterization of atomic layer deposited La_2O_3 films on $In_{0.53}Ga_{0.47}As$ substrates, ECS Trans. 58 (2013) 385–389.
[5] J. Zhang, X. Lou, M. Si, H. Wu, J. Shao, M.J. Manfra, R.G. Gordon, P.D. Ye, Inversion-mode GaAs wave-shaped field-effect transistor on GaAs (100) substrate, Appl. Phys. Lett. 106 (2015) 073506.
[6] I.-K. Oh, M.-K. Kim, J.-S. Lee, C.-W. Lee, C. Lansalot-Matras, W. Noh, J. Park, A. Noori, D. Thompson, S. Chu, W.J. Maeng, H. Kim, The effect of La_2O_3-incorporation in HfO_2 dielectrics on Ge substrate by atomic layer deposition, Appl. Surf. Sci. 287 (2013) 349–354.
[7] X. Wang, L. Dong, J. Zhang, Y. Liu, P.D. Ye, R.G. Gordon, Heteroepitaxy of La_2O_3 and $La_{2-x}Y_xO_3$ on GaAs (111)A by atomic layer deposition: achieving low interface trap density, Nano Lett. 13 (2013) 594–599.
[8] S. Kamiyama, T. Miura, E. Kurosawa, Band edge gate first HfSiON/metal gate n-MOSFETs using ALD-La_2O_3 cap layers scalable to EOT = 0.68 nm for 32 nm bulk devices with high performance and reliability, Technical Digest of the International Electron Devices Meeting (IEDM), 2007, pp. 539–542.
[9] D. Lim, W.S. Jung, Y.J. Kim, C. Choi, Electrical characteristics of ALD La_2O_3 capping layers using different lanthanum precursors in MOS devices with ALD HfO_2, $HfSiO_x$, and HfSiON gate dielectrics, Microelectron. Eng. 147 (2015) 206–209.
[10] R. Boujamaa, E. Martinez, F. Pierre, O. Renault, B. Detlefs, J. Zegenhagen, S. Baudot, M. Gros-Jean, F. Bertin, C. Dubourdieu, Study of the La-related dipole in TiN/LaO_x/HfSiON/SiON/Si gate Stacks using hard X-ray photoelectron spectroscopy and backside medium energy ion scattering, Appl. Surf. Sci. 335 (2015) 71–77.
[11] G. Mavrou, S. Galata, P. Tsipas, A. Sotiropoulos, Y. Panayiotatos, A. Dimoulas, E.K. Evangelou, J.W. Seo, C. Dieker, Electrical properties of La_2O_3 and HfO_2/La_2O_3 gate dielectrics for germanium metal-oxide-semiconductor devices, J. Appl. Phys. 103 (2008) 014506.
[12] X.-F. Li, X.-J. Liu, Y.-Q. Cao, A.-D. Li, H. Li, D. Wu, Improved interfacial and electrical properties of atomic layer deposition HfO_2 films on Ge with La_2O_3 passivation, Appl. Surf. Sci. 264 (2013) 783–786.
[13] L. Lamagna, C. Wiemer, S. Baldovino, A. Molle, M. Perego, S. Schamm-Chardon, P.E. Coulon, M. Fanciulli, Thermally induced permittivity enhancement in La-doped ZrO_2 grown by atomic layer deposition on Ge(100), Appl. Phys. Lett. 95 (2009) 122902.
[14] Y.-M. Gao, P. Wu, K. Dwight, A. Wold, Growth and characterization of thin films of Y_2O_3, La_2O_3, and La_2CuO_4, J. Solid State Chem. 90 (1991) 228–233.
[15] J.W. Fergus, Oxide materials for high temperature thermoelectric energy conversion, J. Eur. Ceram. Soc. 32 (2012) 525–540.
[16] Y. Zhao, M. Toyama, K. Kita, K. Kyuno, A. Toriumi, Moisture-absorption-induced permittivity deterioration and surface roughness enhancement of lanthanum oxide films on silicon, Appl. Phys. Lett. 88 (2006) 072904.
[17] B.S. Lim, A. Rahtu, P. de Rouffignac, R.G. Gordon, Atomic layer deposition of lanthanum aluminum oxide nano-laminates for electrical applications, Appl. Phys. Lett. 84 (2004) 3957–3959.
[18] M. Suzuki, T. Yamaguchi, N. Fukushima, M. Koyama, $LaAlO_3$ gate dielectric with ultrathin equivalent oxide thickness and ultralow leakage current directly deposited on Si substrate, J. Appl. Phys. 103 (2008) 034118.
[19] S. Wang, H. Liu, H. Zhang, The influence of La/Al atomic ratio on the dielectric constant and band-gap of stack-gate La–Al–O/SiO_2 structure, J. Mater. Sci. Mater. Electron. 28 (2017) 2004–2008.
[20] M. Ritala, M. Leskelä, Atomic layer deposition, in: H.S. Nalwa (Ed.), Deposition and Processing of Thin Films; Handbook of Thin Film Materials, Vol. 1 Academic Press, San Diego, CA, 2002, pp. 103–159.
[21] M. Nieminen, M. Putkonen, L. Niinistö, Formation and stability of lanthanum oxide thin films deposited from β-diketonate precursor, Appl. Surf. Sci. 174 (2001) 155–165.
[22] D. Tsoutsou, G. Scarel, A. Debernardi, S.C. Capelli, S.N. Volkos, L. Lamagna, S. Schamm, P.E. Coulon, M. Fanciulli, Infrared spectroscopy and X-ray diffraction studies on the crystallographic evolution of La_2O_3 films upon annealing, Microelectron. Eng. 85 (2008) 2411–2413.
[23] W.-H. Kim, W.J. Maeng, K.-J. Moon, J.-M. Myoung, H. Kim, Growth characteristics and electrical properties of La_2O_3 gate oxides grown by thermal and plasma-enhanced atomic layer deposition, Thin Solid Films 519 (2010) 362–366.
[24] B. Lee, T.J. Park, A. Hande, M.J. Kim, R.M. Wallace, J. Kim, X. Liu, J.H. Yi, H. Li, M. Rousseau, D. Shenai, J. Suydam, Electrical properties of atomic-layer-deposited La_2O_3 films using a novel La formamidinate precursor and ozone, Microelectron. Eng. 86 (2009) 1658–1661.
[25] K. Kukli, M. Ritala, V. Pore, M. Leskelä, T. Sajavaara, R.I. Hegde, D.C. Gilmer, P.J. Tobin, A.C. Jones, H.C. Aspinall, Atomic layer deposition and properties of lanthanum oxide and lanthanum-aluminum oxide films, Chem. Vap. Depos. 12 (2006) 158–164.
[26] J. Niinistö, Atomic Layer Deposition of High-κ Dielectrics From Novel Cyclopentadienyl-type Precursors (Ph.D. Thesis), Helsinki University of Technology, Finland, 2006.
[27] S. Seppälä, J. Niinistö, T. Blanquart, M. Kaipio, K. Mizohata, J. Räisänen, C. Lansalot-Matras, W. Noh, M. Ritala, M. Leskelä, Heteroleptic cyclopentadienyl-amidinate precursors for atomic layer deposition (ALD) of Y, Pr, Gd, and Dy oxide thin films, Chem. Mater. 28 (2016) 5440–5449.
[28] M. Ylilammi, T. Ranta-aho, Optical determination of the film thicknesses in multilayer thin film structures, Thin Solid Films 232 (1993) 56–62.
[29] M. Vehkamäki, T. Hatanpää, M. Ritala, M. Leskelä, S. Väyrynen, E. Rauhala, Atomic layer deposition of $BaTiO_3$ thin films – effect of barium hydroxide formation, Chem. Vap. Depos. 13 (2007) 239–246.
[30] Y.K. Kim, B.D. Kay, J.M. White, Z. Dohnalek, Inductive effect of alkyl chains on alcohol dehydration at bridge-bonded oxygen vacancies of TiO2(110), Catal. Lett. 119 (2007) 1–4.
[31] J.F. DeWilde, H. Chiang, D.A. Hickman, C.R. Ho, A. Bhan, Kinetics and mechanism of ethanol dehydration on γ-Al_2O_3: the critical role of dimer inhibition, ACS Catal. 3 (2013) 798–807.
[32] P. Kostestkyy, J. Yu, R.J. Gorte, G. Mpourmpakis, Structure–activity relationships on metal oxides: alcohol dehydration, Cat. Sci. Technol. 4 (2014) 3861–3869.
[33] M.P. Rosynek, R.J. Koprowski, G.N. Dellisante, The nature of catalytic sites on lanthanum and neodymium oxides for dehydration/dehydrogenation of ethanol, J. Catal. 122 (1990) 80–94.
[34] S. Schamm, P.E. Coulon, S. Miao, S.N. Volkos, L.H. Lu, L. Lamagna, C. Wiemer, D. Tsoutsou, G. Scarel, M. Fanciulli, Chemical/structural nanocharacterization and electrical properties of ALD-grown La_2O_3/Si interfaces for advanced gate stacks, J. Electrochem. Soc. 156 (2009) H1–H6.
[35] J. Niinistö, N. Petrova, M. Putkonen, L. Niinistö, T. Sajavaara, Gadolinium oxide thin films by atomic layer deposition, J. Cryst. Growth 285 (2005) 191–200.